A reactive center loop–based prediction platform to enhance the design of therapeutic SERPINs

Wariya Sanrattana[a], Thibaud Sefiane[b], Simone Smits[a], Nadine D. van Kleef[a], Marcel H. Fens[c], Peter J. Lenting[b], Coen Maas[a], and Steven de Maat[a,1]

[a]Department of Clinical Chemistry and Haematology, University Medical Center Utrecht, Utrecht University, Utrecht 3584, The Netherlands; [b]Laboratory for Haemostasis, Inflammation and Thrombosis, INSERM, Unité Mixte de Recherche 1176, Université Paris-Saclay 94276 Le Kremlin-Bicêtre, France; and [c]Utrecht Institute for Pharmaceutical Sciences, Utrecht University, Utrecht 3584, The Netherlands

Edited by Charles S. Craik, University of California, San Francisco, CA, and accepted by the Editorial Board September 24, 2021 (received for review May 5, 2021)

Serine proteases are essential for many physiological processes and require tight regulation by serine protease inhibitors (SERPINs). A disturbed SERPIN–protease balance may result in disease. The reactive center loop (RCL) contains an enzymatic cleavage site between the P1 through P1′ residues that controls SERPIN specificity. This RCL can be modified to improve SERPIN function; however, a lack of insight into sequence–function relationships limits SERPIN development. This is complicated by more than 25 billion mutants needed to screen the entire P4 to P4′ region. Here, we developed a platform to predict the effects of RCL mutagenesis by using α1-antitrypsin as a model SERPIN. We generated variants for each of the residues in P4 to P4′ region, mutating them into each of the 20 naturally occurring amino acids. Subsequently, we profiled the reactivity of the resulting 160 variants against seven proteases involved in coagulation. These profiles formed the basis of an in silico prediction platform for SERPIN inhibitory behavior with combined P4 to P4′ RCL mutations, which were validated experimentally. This prediction platform accurately predicted SERPIN behavior against five out of the seven screened proteases, one of which was activated protein C (APC). Using these findings, a next-generation APC-inhibiting α1-antitrypsin variant was designed (KMPR/RIRA; / indicates the cleavage site). This variant attenuates blood loss in an in vivo hemophilia A model at a lower dosage than the previously developed variant AIKR/KIPP because of improved potency and specificity. We propose that this SERPIN-based RCL mutagenesis approach improves our understanding of SERPIN behavior and will facilitate the design of therapeutic SERPINs.

SERPIN | hemophilia | protein engineering

The superfamily of serine proteases is essential for human physiology in processes such as coagulation, fibrinolysis, inflammation, and immunity. They are produced in a resting zymogen form. Upon activation, their enzymatic activity increases tremendously (1). Excessive serine protease activity can cause disease; hence, they require tight regulation by physiological inhibitors.

Serine protease inhibitors (SERPINs) are a superfamily of inhibitors found throughout all the kingdoms of life. SERPINs have a conserved inhibitory mechanism. They target only active serine proteases (i.e., not zymogens) and often have the ability to inhibit multiple proteases within a biological mechanism. SERPIN specificity is predominantly determined via their reactive center loop (RCL) (2, 3). The RCL is a flexible loop that acts as a substrate. Upon RCL cleavage at the reactive center between the P1 and P1′ residues, the SERPIN undergoes a rapid conformational change, integrating the N-terminal part of the RCL into its core structure (4, 5). If this occurs during the intermediate step of the cleavage process (when the protease is covalently bound to the N-terminal part of the RCL), the protease is dragged along during the conformational change of the SERPIN (6). As a result, the active site of the protease becomes distorted and loses its enzymatic activity. Subsequently, the stable protease–SERPIN complex is then marked for destruction (7).

Alterations to the RCL sequence can have a dramatic impact on the SERPIN function or specificity. For instance, wild-type α1-antitrypsin (α1AT-WT) is a potent inhibitor of neutrophil elastase, whereas the rare pathogenic Pittsburgh mutation (at P1 residue: $M^{358}R$; α1AT-Pittsburgh) alters its specificity completely. α1AT-Pittsburgh no longer inhibits elastase (8) but has become a potent broad specificity inhibitor of proteases, which prefer arginine or lysine as a P1 residue (9). This includes coagulation proteases (e.g., thrombin, activated factor X [FXa], and activated factor XI [FXIa]) as well as anticoagulant or profibrinolytic proteases (e.g., activated protein C [APC] and plasmin), resulting in a bleeding phenotype (10).

Alignment of human SERPIN RCL sequences reveals that the N-terminal region is conserved among inhibitory SERPINs, suggesting that this region is important to maintain proper RCL mobility and loop insertion. In contradiction, the sequences adjacent to the cleavage site in the RCL, particularly residues spanning from P4 to P4', are highly variable between different SERPINs and are thought to be a major determinant of SERPIN specificity (2, 11). The possibility to alter and fine-tune SERPIN specificity via RCL modification encourages their development as therapeutic agents. However, the design of specific RCL sequences has its challenges.

Significance

Serine protease inhibitors (SERPINs) regulate vital physiological processes. Considerable research effort has gone into the development of SERPINs as therapeutic agents. One of the development goals is SERPIN modification for improved specificity toward desired target(s). The specificity and potency of SERPINs can be altered by changing their reactive center loop (RCL). Currently, predicting these properties of a RCL sequence is almost impossible. By characterizing 160 α1-antitrypsin RCL variants with single–amino acid substitutions, we developed a SERPIN RCL-based platform that predicts the inhibitory behavior for SERPIN variants with compounded RCL mutations. This platform was applied to design a next-generation SERPIN against activated protein C and provides evidence for its value in the treatment of hemophilia A.

Author Contributions: W.S., C.M., and S.d.M. designed the research; W.S., T.S., S.S., N.D.v.K., and S.d.M. performed research; M.H.F. and P.J.L. contributed new reagents/analytic tools; W.S., T.S., N.D.v.K., C.M., and S.d.M. analyzed data; and W.S., C.M., and S.d.M. wrote the paper.

The authors declare no competing interest.

This article is a PNAS Direct Submission. C.S.C. is a guest editor invited by the Editorial Board.

[1]To whom correspondence may be addressed. Email: s.demaat@umcutrecht.nl.

This article contains supporting information online at http://www.pnas.org/lookup/suppl/doi:10.1073/pnas.2108458118/-/DCSupplemental.

Published November 5, 2021.

Ideally, the design of a "perfect" SERPIN against a target protease would encompass the functional screening of all conceivable RCL variants (P4 to P4' residues) in a full-length SERPIN backbone. However, this RCL octapeptide represents more than 25 billion possible combinations. This makes the development and functional characterization a challenging undertaking.

Positional scanning synthetic combinatorial libraries (PS-SCL; reflecting PX to P1 residues but not P' residues) are powerful tools to gain insights into the sequence–function relationship of SERPIN RCLs (12, 13). These libraries allow for the rapid interrogation of serine protease specificity, but have limitations (14, 15), such as issues with the cooperativity of neighboring interactions (reviewed in ref. 16) or the contributions of the essential P' residues (17, 18). As such, grafting these PS-SCL–derived sequences directly onto the RCL of α1AT often does not result in the required specificity (17, 18).

To facilitate therapeutic SERPIN design, we here report the development of an SERPIN-based platform to help predict RCL specificity. Hereto, 160 RCL variants were created with α1AT-Pittsburgh as a template because of its broad and potent inhibitory profile. These variants were divided into eight SERPIN RCL libraries representing each of the eight residues within the P4 to P4' area. The libraries were profiled against seven coagulation proteases, and outcomes were compounded into an RCL-scoring system. Using this platform, next-generation α1AT variants were developed against APC, demonstrating improved efficacy and specificity, compared to a previously published variant. Finally, the lead candidate was validated in an in vivo model of hemophilia A.

Results

Predicting RCL Specificity. To develop a prediction model for SERPIN specificity that consists of a manageable number of variants, we set out to identify the contribution of each of the individual residues within the RCL P4 to P4' sequence. Hereto, α1AT-Pittsburgh was chosen as a template RCL sequence (AIPR/SIPP; / indicates the reactive center) because of its broad and potent inhibitory profile. A total number of 160 α1AT variants were generated, spanning the P4 to P4' area (Fig. 1*A*). Each of the eight libraries represents a single, individual RCL position, to which each of the 20 different, naturally occurring amino acids were introduced. The α1AT variants were expressed in human embryonic kidney (HEK) 239F cells, and secreted α1AT protein levels were equalized by densitometric analysis of Coomassie-stained SDS-PAGE (sodium dodecyl sulphate–polyacrylamide gel electrophoresis) gels prior to inhibition experiments (*SI Appendix*, Fig. S1*A*). Their inhibitory capacity was screened against seven proteases involved in coagulation: thrombin, FXa, FXIa, APC, plasmin, activated factor XII (FXIIa), and plasma kallikrein (PKa). Hereto, α1AT variants were preincubated with each of these proteases for 5 min. Subsequently, residual protease activity was measured (*SI Appendix*, Fig. S1*B*). Residual protease activity was normalized and expressed as 0 to 100% inhibition, in which vehicle (no inhibition) was set to 0%, and the most potent α1AT variant (under nonsaturating conditions) within the library was set to 100% (*SI Appendix*, Fig. S1*C*). Outcomes of these inhibitory assays are summarized as a heat map for each protease (Fig. 1 *B–H*). As expected for these trypsin-like serine proteases, all favor an arginine (R) at P1, with thrombin, FXIa and plasmin also showing inhibition when lysine (K) is present at P1. At the other RCL positions, proteases show distinct profiles. When incomplete protease inhibition was seen in these experiments, it can either be the result of differences in kinetics or because of the consumption of the SERPIN as a substrate (reviewed in ref. 2).

We went on to develop an in silico model to predict the combined effects of multiple RCL mutations. Hereto, normalized data from the inhibition studies (Fig. 1 *B–H*) for amino acid variation at each RCL position were compounded. This approach allows for the generation of a predicted inhibition score ranging between 0 and 100%, per protease, for any P4 to P4' sequence. In a similar fashion, we developed a prediction model based on historical PS-SCL studies (12, 13).

We selected the top 10 RCL sequences predicted by either our SERPIN RCL-based prediction algorithm or the PS-SCL–based prediction algorithm, alongside the top 10 of RCL sequences that showed the biggest discrepancy in prediction between both libraries. Duplicate sequences were excluded (*SI Appendix*, Fig. S2*A* and *SI Appendix*, Table S2). As a result, 17 to 25 unique variants were selected for each of the target proteases.

These α1AT RCL variants were produced and investigated experimentally (Fig. 2). We found strong and significant correlations between the predicted and actual behavior for FXIIa, thrombin, and APC (R^2: 0.8049, 0.7287, and 0.7248, respectively), when our SERPIN RCL-based prediction model was applied (Fig. 2 *A–C*). Moderate correlations were observed for FXIa and plasmin (Fig. 2 *D* and *E*), but no significant correlations were found for PKa and FXa (Fig. 2 *F* and *G*). In comparison, for the PS-SCL predictions, only thrombin and FXIa showed weak but significant correlations (R^2: 0.3954 and 0.2178; Fig. 2 *B* and *D*). Overall, these data show that while the SERPIN RCL-based prediction platform is not completely predictive (five out of seven proteases), it is a step forward compared to the prediction based upon PS-SCL data and should aid in the development of therapeutic SERPINs.

Design of a Next-Generation, APC-Specific α1-Antitrypsin. In 2017, Polderdijk et al. published the development of α1AT variants for the specific inhibition of APC as a treatment for hemophilia (18). Based upon the protein crystal structures of thrombin and APC, the P2 to P1' residues of RCL of α1AT-Pittsburgh were redesigned to KRK (α1AT-KR/K; / indicates the reactive center). In murine models of hemophilia B, α1AT-KR/K restores the bleeding phenotype in a dose-dependent manner. Using the random mutagenesis of the P2 and P1' position, more APC inhibitors were developed (19). While these new variants (α1AT-RR/Q and α1AT-KR/Q) showed similar specificity, their capacity to inhibit APC was ∼1.6-fold lower than α1AT-KR/K. This excellent work demonstrated the difficulty in tailoring SERPIN specificity. Using our prediction platform, we set out to develop a next-generation APC inhibitor. Our platform predicted KMPR/SIPA (P4 to P4') to be the most potent APC inhibitor, but showed broad specificity (*SI Appendix*, Fig. S3*A*). Subsequently, we tailored this template RCL sequence in a stepwise manner to improve predicted specificity while maintaining APC inhibition (*SI Appendix*, Fig. S3*B*). This approach identified a family of three RCL sequences: KMPR/RIRA, KIPR/RIRA, and KRPR/RIRA. These variants were predicted to inhibit APC at least 2.7-fold stronger than the KR/K sequence while maintaining or improving specificity (i.e., the decreased inhibition of thrombin, FXa, FXIa, plasmin, FXIIa, and PKa; *SI Appendix*, Fig. S3*B*). We produced these α1AT variants alongside α1AT-WT, α1AT-Pittsburgh, and α1AT-KR/K as controls and references.

In the buffer, α1AT-KMPR/RIRA, -KIPR/RIRA, and -KRPR/RIRA showed the improved inhibition of APC, compared to α1AT-KR/K with a 3.9-, 4.5- and 1.6-fold increase in second-order rate constants (k_2), respectively (Fig. 3*A*). For thrombin and FXa, inhibition was negligible (i.e., well below that of α1AT-WT and almost equal to α1AT-KR/K (Fig. 3 *B* and *C*) with k_2 values in the 10 $M^{-1} \cdot s^{-1}$ range. α1AT-KMPR/RIRA, -KIPR/RIRA, and -KRPR/RIRA inhibited FXIa 9.5-,

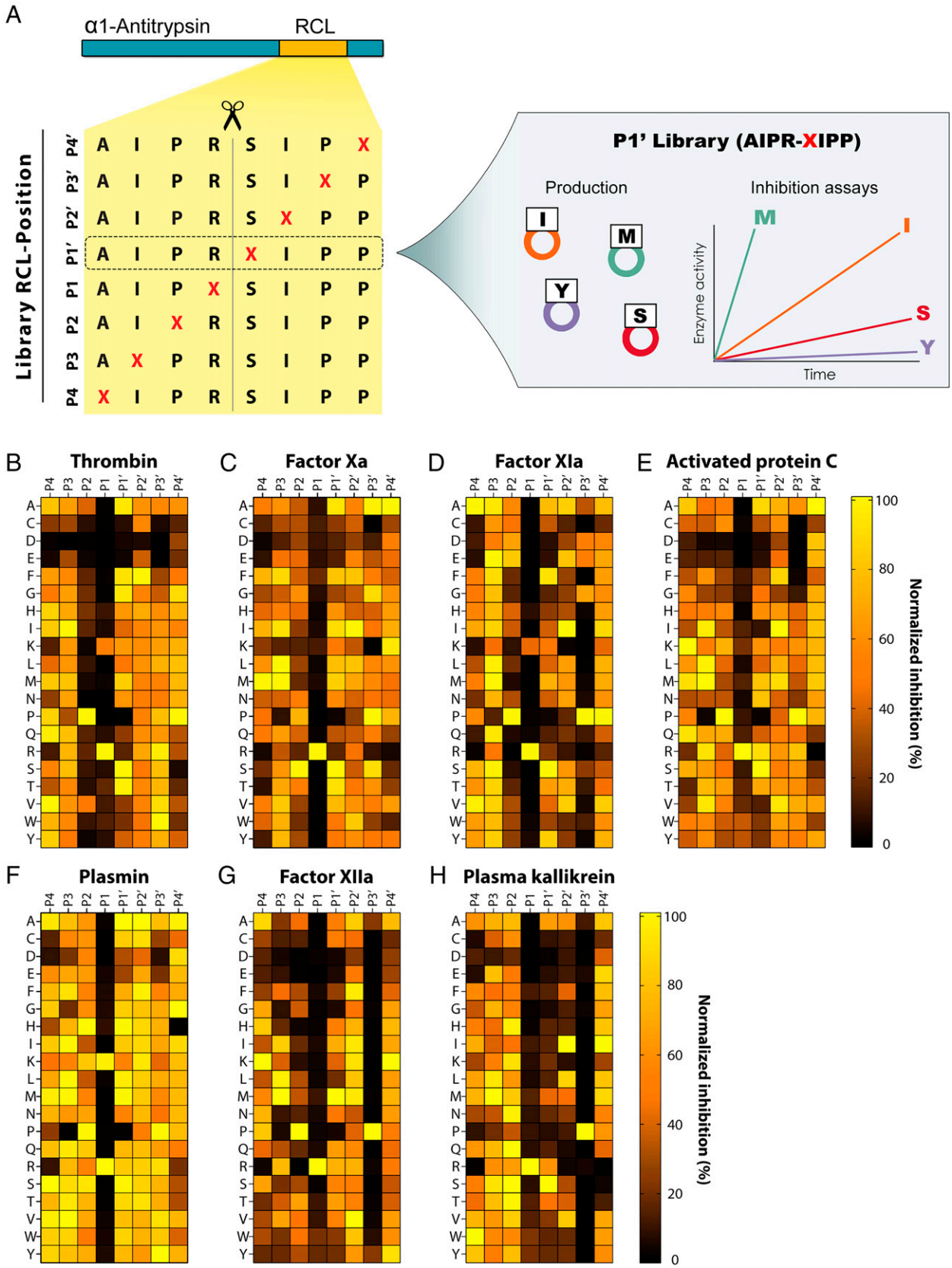

Fig. 1. Platform development and functional characterization of 160 α1-antitrypsin RCL variants against seven coagulation proteases. (*A*) Strategy. Eight independent libraries (from P4 to P4′) were created to identify the contribution of all naturally occurring amino acids to the inhibitory profile. The RCL sequence of α1AT-Pittsburgh was used as a template. (*B–H*) Heat map representations (mean of $n = 3$) for the capacity of SERPIN variants to inhibit various proteases. Strong (100%) inhibition is indicated as yellow; no inhibition (0%) is indicated in black.

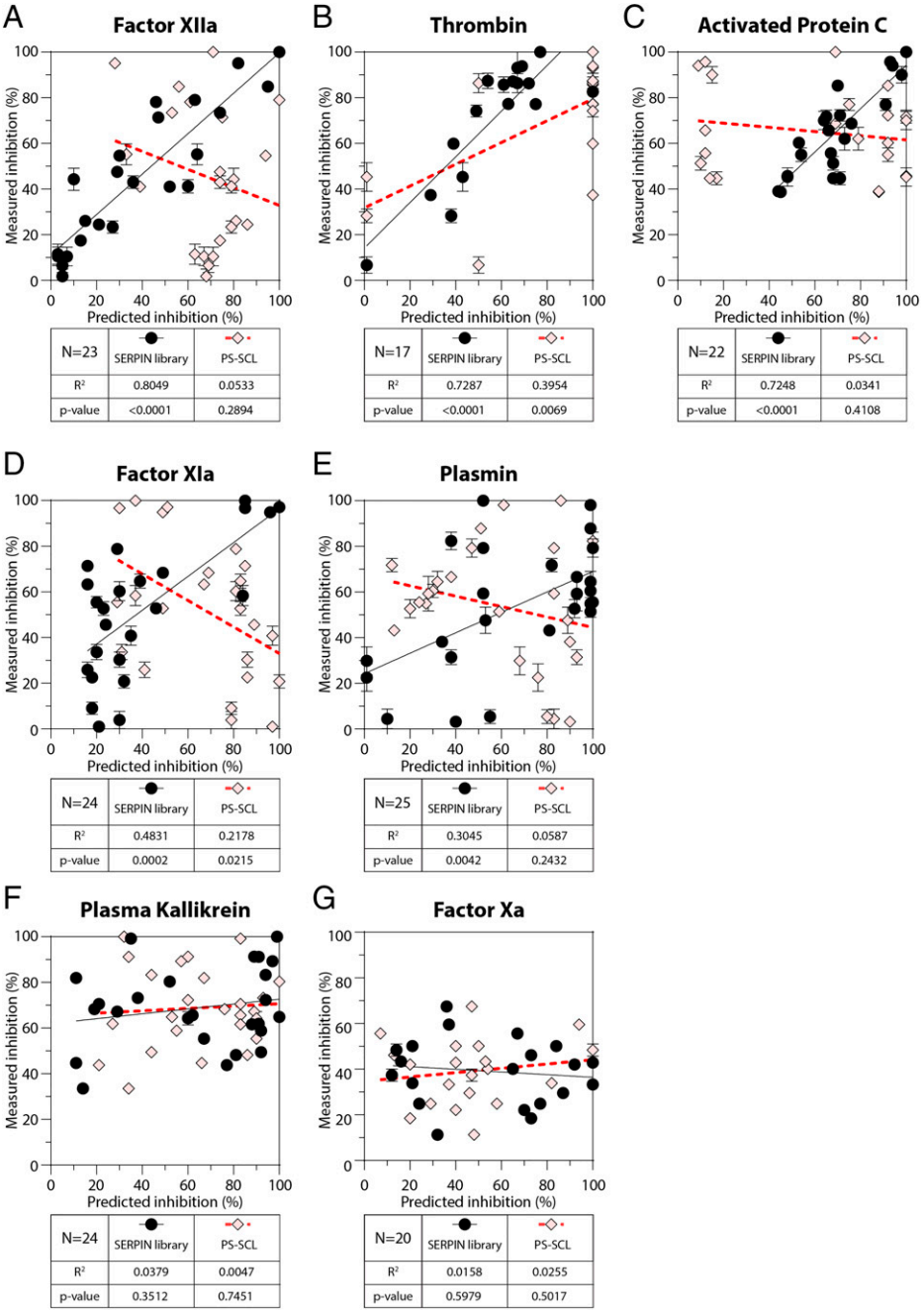

Fig. 2. SERPIN RCL-based predictions are superior to PS-SCL–based predictions for SERPIN development. (*A*–*G*) For each protease, a test cohort (17 to 25 variants) was created to investigate sequence–function relationships. Outcomes were compared to predicted inhibitory inferred from either the SERPIN RCL libraries or PS-SCL. For comparison, only P3 and P2 were varied (P1 = R), as PS-SCL are limited in length. Data represents the mean ± SD from $n = 3$. Correlation and significance were calculated by simple linear regression.

9.5-, and 5.4-fold less than α1AT-KR/K, indicating improved specificity (Fig. 3*D*). As our platform predicted, α1AT-KR/K was a surprisingly potent plasmin inhibitor with a k_2 of 1.27×10^5 $M^{-1} \cdot s^{-1}$ (Fig. 3*E* and *SI Appendix*, Fig. S3*B*). By comparison, α1AT-KMPR/RIRA, -KIPR/RIRA, and -KRPR/RIRA inhibited plasmin 24.7-, 2.4-, and 2.6-fold less strongly than α1AT-KR/K. In similar manner, α1AT-KR/K strongly inhibited PKa with a k_2 of 1.03×10^5 $M^{-1} \cdot s^{-1}$. By comparison, α1AT-KMPR/RIRA, -KIPR/RIRA, and -KRPR/RIRA inhibited PKa 49.7, 72.3, and 42.4-fold less strongly (Fig. 3*F*). In contrast, α1AT-KR/K inhibited FXIIa approximately ninefold less than the three new variants (Fig. 3*G*). These data demonstrate that new RCL variants can be designed with an improved efficacy/specificity profile.

Effects of Next-Generation, APC-Specific α1AT Variants on Plasma Coagulation. Tissue factor (TF) initiates the activation of the extrinsic pathway of the coagulation cascade. This results in the activation of prothrombin into thrombin which allows for fibrin formation, causing plasma to clot (20, 21). In the presence of thrombomodulin, thrombin can also efficiently activate protein C into APC (22). This anticoagulant protease inactivates activated factor VIII (FVIII) and activated factor V (FV) to decrease the rate of thrombin generation. Polderdijk et al.,

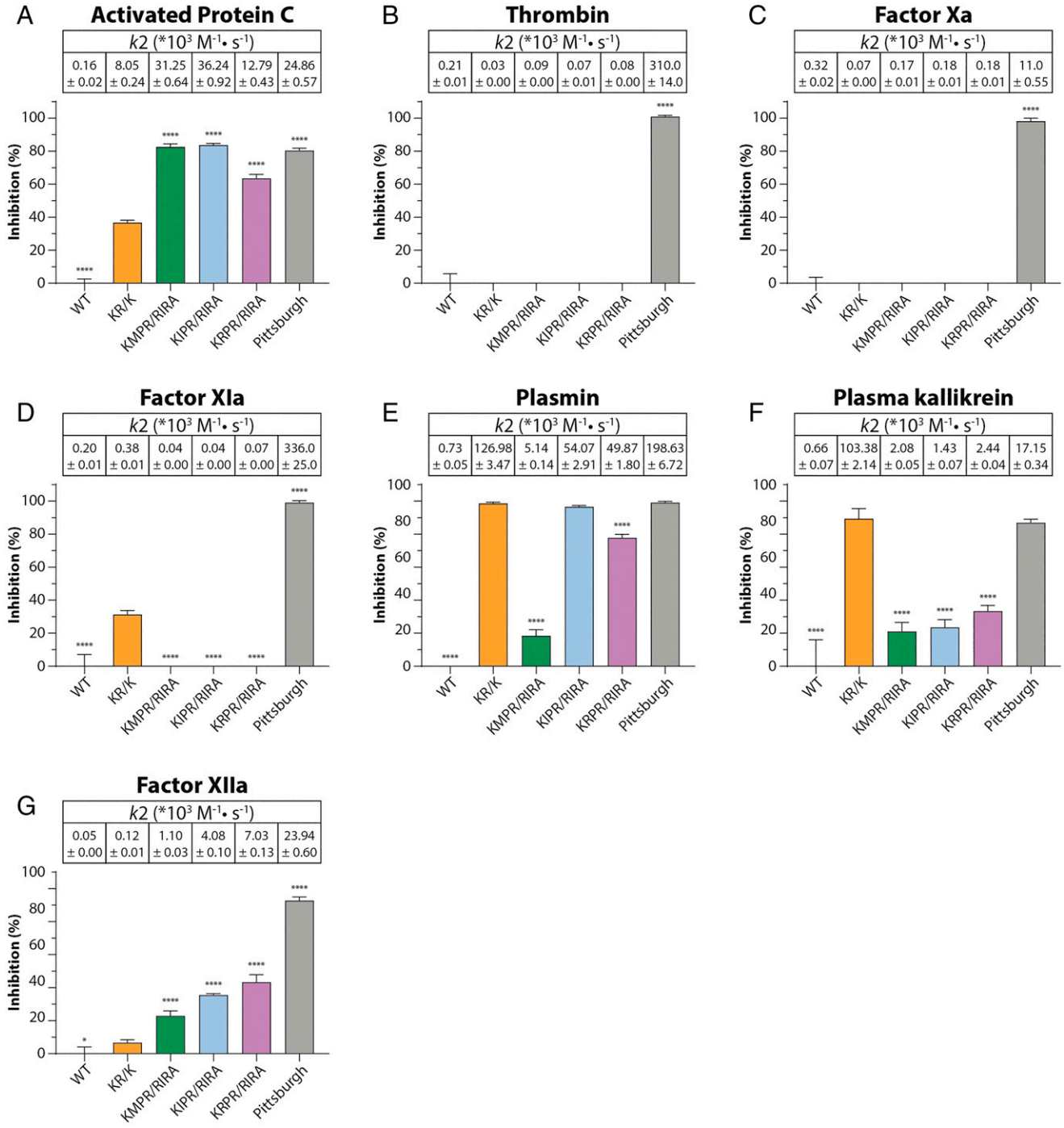

Fig. 3. Development of α1-antitrypsin variants for the strong and specific inhibition of APC. The inhibition screening of APC and other coagulation proteases by α1AT variants; table inset shows second-order rate constants (k_2: $*10^3$ $M^{-1} \cdot s^{-1}$). (*A*) Inhibition of 17.8 nM APC by 96.2 nM SERPIN after 5 min preincubation. (*B*) Inhibition of 8.89 nM thrombin by 38.5 nM SERPIN after 30 min preincubation. (*C*) Inhibition of 8.7 nM factor Xa by 192.3 nM SERPIN after 30 min of preincubation. (*D*) Inhibition of 2.5 nM factor XIa by 9.6 nM SERPIN after 30 min of preincubation. (*E*) Inhibition of 24.1 nM plasmin by 100 nM SERPIN after 30 min of preincubation. (*F*) Inhibition of 1 nM PKa by 50 nM SERPIN after 30 min of preincubation. (*G*) Inhibition of 25 nM factor XIIa by 100 nM SERPIN after 30 min of preincubation. Data represents the mean ± SD of three separate experiments, each performed in duplicate. $*P < 0.05$ and $****P < 0.0001$ compared to α1AT-KR/K by one-way ANOVA with post hoc Dunnett's multiple comparison test.

showed that APC inhibition attenuates defective thrombin generation in hemophilia A or B plasma (deficient in FVIII or factor IX [FIX], respectively) (18).

We next investigated our α1AT variants in plasma coagulation assays. In the absence of thrombomodulin (no APC activation), α1AT-WT, α1AT-KR/K, and our three α1AT variants did not influence thrombin generation, even in concentrations up to 2 μM (Fig. 4 *A*–*C*). Neither the maximum concentration of thrombin formed (peak height) nor the endogenous thrombin potential (ETP) was influenced (*SI Appendix*, Figs. S5, S9, and S12). In contrast, α1AT-Pittsburgh, which is a known thrombin inhibitor, dose dependently decreased thrombin generation. These observations match those seen in diluted TF-driven prothrombin (PT) clotting assays (*SI Appendix*, Fig. S4*A*).

Remarkably, when coagulation was induced via the intrinsic pathway (dilute partial thromboplastin time [aPTT] assay), both α1AT-KR/K and -KRPR/RIRA showed a minor, but significant, prolongation of the clotting time compared to α1AT-WT (*SI Appendix*, Fig. S4*B*). This observation may correspond to the residual FXIIa, FXIa, or PKa inhibition of these α1AT variants (Fig. 3 *D, F* and *G*). Nonetheless, the prolongation of the clotting time was not to the extent of that of α1AT-Pittsburgh (2.7-fold longer than α1AT-WT).

In the presence of 1.25 nM thrombomodulin, the thrombin potential was lowered by ∼50% because of APC activation. As previously reported, α1AT-KR/K partially reversed the anticoagulant effect of thrombomodulin on thrombin generation both in normal plasma, as well as FVIII- and FIX-deficient plasmas (Fig. 4 *D–F*, respectively; *SI Appendix*, Figs. S6, S10, and S13). Here, α1AT-KR/K reached a maximum ETP restoration (E_{max}) of 74.1% (±11.4%) (vehicle remains 50%). A concentration of 202.2 (±38.6) nM of α1AT-KR/K was required to reach half of the maximum effect (EC_{50}) (*SI Appendix*, Table S6). By comparison, α1AT-KMPR/RIRA almost fully restored thrombin potential with an E_{max} of 92.8% (±0.5%) and an EC_{50} of 120.7 (±18.8) nM. For α1AT-KIPR/RIRA, but not α1AT-KRPR/RIRA, a similar significant improvement was observed (E_{max} 94.3% [±2.3%] and EC_{50} 74.3 [±12.9] nM). Similar results were found in normal plasma at higher-thrombomodulin concentrations (Fig. 4 *G* and *J* and *SI Appendix*, Figs. S7 and S8). Even at 10 nM of thrombomodulin, α1AT-KMPR/RIRA and -KIPR/RIRA strongly restored thrombin potential (Fig. 4*J* and *SI Appendix*, Table S6). We analyzed protease–SERPIN complexes by Western blotting and found that the SERPIN variants that were most capable of restoring thrombin potential formed more complex with APC (*SI Appendix*, Fig. S15 *A* and *B*). This was accompanied by increased prothrombin and FX activation (i.e., consumption of single-chain zymogen and formation of thrombin–antithrombin complex) (*SI Appendix*, Fig. S15 *C–E*). We observed no protease–SERPIN complexes for FVIIa, FIXa, FXIa, or FXIIa during coagulation, confirming the specificity of our α1AT variants.

In FVIII-deficient plasma, in the presence of thrombomodulin (Fig. 4 *E* and *H* and *SI Appendix*, Figs. S10 and S11), α1AT-KMPR/RIRA, -KIPR/RIRA and -KRPR/RIRA significantly increased the E_{max} (15 to 40% higher than α1AT-KR/K), while their EC_{50} were lower than that of α1AT-KR/K by at least 20% (*SI Appendix*, Table S6). These differences between α1AT-KR/K and the three novel variants were smaller in FIX-deficient plasma (Fig. 4 *F* and *I* and *SI Appendix*, Figs. S13 and S14), which is in line with the previous finding that α1AT-KR/K performed better in FIX-deficient plasma than in FVIII-deficient plasma (15).

Next, we studied the behavior of our SERPIN variants during fibrinolysis in plasma clot lysis turbidity assays (*SI Appendix*, Fig. S16). Hereto, we triggered coagulation (increases turbidity) in the presence of tissue plasminogen activator (tPA), resulting in fibrinolysis (decreases turbidity). In the absence of thrombomodulin, neither clot formation nor fibrinolysis was affected by any of the SERPINs, with α1AT-Pittsburgh as the only exception (*SI Appendix*, Fig. S16 *A–C*, *G–I*, and *M–O*). In the presence of thrombomodulin, coagulation was delayed as expected. This was unaffected by the SERPIN variants, again with α1AT-Pittsburgh as exception (*SI Appendix*, Fig. S16 *D–E*, *J–K*, and *P–Q*). Interestingly, clot lysis times were prolonged in normal pooled plasma and FVIII-deficient plasma in the presence of α1AT-KR/K and the three novel variants (*SI Appendix*, Fig. S16 *F, L*, and *R*). This prolongation appears to be associated rather with their capacity to inhibit APC than plasmin (Fig. 3 *A* and *E*). During clot lysis, in the absence of thrombomodulin, plasmin formed ∼140 kDa complexes with all recombinant SERPINs (under nonreducing conditions: detection antibody recognizes plasmin heavy chain) (*SI Appendix*, Fig. S17 *A* and *B*) but in particular in the presence of KR/K or KIPR/RIRA. Under reducing conditions, all recombinant SERPINs except for WT formed ∼80 kDa complexes (*SI Appendix*, Fig. S17 *C* and *D*). α1AT-Pittsburgh formed these complexes in the absence, but not in the presence, of thrombomodulin. None of the SERPIN variants were cross-reactive for tPA or PKa (*SI Appendix*, Fig. S17 *E* and *F*), despite their involvement during thrombolysis (23).

Finally, we set out to validate the efficacy of our SERPINS in a mouse model for hemophilia A (FVIII-deficient mice on a C57BL/6 background). First, we confirmed that α1AT-KMPR/RIRA (our lead compound) and α1AT-KR/K are able to improve thrombin generation in mouse plasma in the presence of thrombomodulin (*SI Appendix*, Fig. S18). Also here, the new SERPIN variant was more potent than α1AT-KR/K.

FVIII-deficient mice were pretreated with saline (negative vehicle control), FVIII (positive control), or α1AT variants via intravenous injection 5 min prior to tail-clip injury, after which blood loss was monitored (Fig. 4*K*). Whereas FVIII administration fully corrected the bleeding defect, α1AT-WT was unable to do so. Only at 15 mg/kg, α1AT-KR/K was able to partially restore blood loss to a median of 363 μL/30 min. By comparison, α1AT-KMPR/RIRA treatment already significantly reduced blood loss at 7.5 mg/kg. It is of note that increasing the dose to 15 mg/kg did not lead to further improvement, suggesting that APC inhibition in hemophilia A can maximally attenuate blood loss by ∼55%. Overall, these data suggest that the rational redesign of therapeutic SERPINs should hold value to increase the therapeutic window for clinical application.

Discussion

The goal of designing SERPIN specificity by changing its RCL sequence has been pursued for decades. Work with RCL chimeras has shown that α1AT specificity is almost completely determined by this sequence (24). Despite these tremendous efforts, insights, and advances in various techniques, designing RCL specificity has remained a challenge. In this project, we first mapped out the contribution of single-RCL residues (Fig. 1) and compounded the data into an in silico prediction platform. Experimental validation studies confirmed that predictions from our SERPIN-based prediction algorithm were better than those from a PS-SCL–based prediction algorithm. However, these were still limited in accuracy for selected proteases (Fig. 2). Prediction accuracy within this model might be limited as it does not incorporate the effect of neighboring amino acids that are present in the three-dimensional structure (25–28). Indeed, earlier studies with recombinant full-length α1AT variants provided evidence for cooperativity between RCL amino acids (24, 29). This may directly affect RCL cleavage, but might also be of influence on the RCL integration into the SERPIN backbone, a process that is essential for SERPIN function. Finally, RCL changes could influence the RCL interplay with its surrounding and local hydrophobicity and electrostatics (3, 30). As such, high-throughput screening [i.e., phage-display (31, 32)], guided by our prediction platform, could help the identification of the correct RCL sequences.

To showcase the applicability of our prediction platform, we developed a next-generation panel of APC-specific α1AT variants. We identified a family of three RCL α1AT variants and selected α1AT-KMPR/RIRA as our lead compound based on efficacy and specificity in in vitro assays (Figs. 3 and 4 *A–J*). In FVIII-deficient mice (hemophilia type A), α1AT-KMPR/RIRA reduced blood loss at 7.5 mg/kg, whereas α1AT-KR/K did not (Fig. 4*K*). Interestingly, we observed no significant improvement at the higher dose of 15 mg/kg α1AT-KMPR/RIRA, while blood loss was only partially (∼55%) restored. This suggests

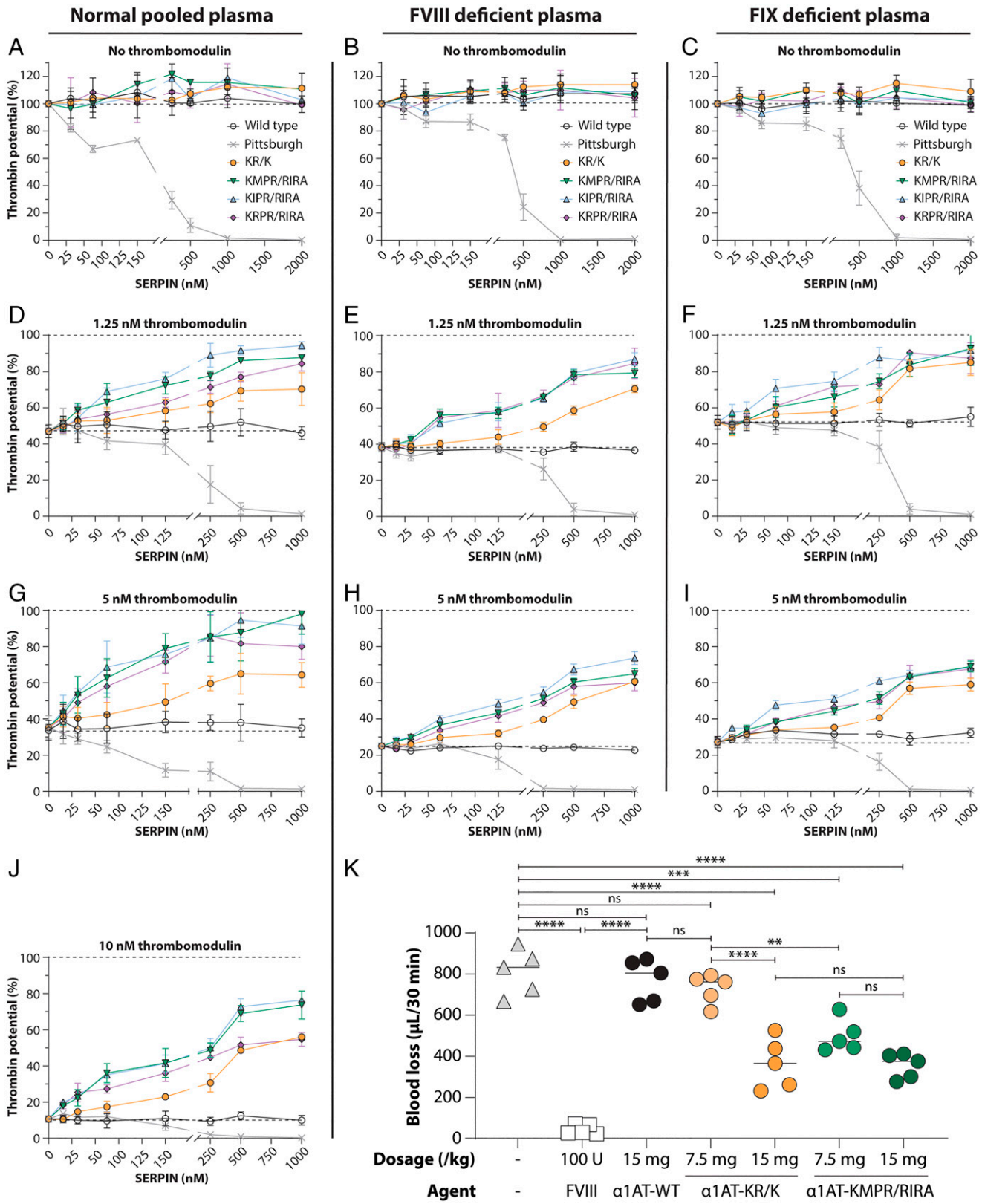

Fig. 4. Next-generation α1-antitrypsin variants that block APC effectively restore defective hemostasis in vitro and in vivo in hemophilia A mice. (*A*–*C*) TF induced thrombin generation in normal pooled plasma (*A*; 0.5 pM), FVIII–deficient plasma (*B*; 1 pM), and FIX-deficient plasma (*C*; 4 pM) in the absence of thrombomodulin. *(D–J)* Effect of SERPINs on TF-driven thrombin generation in the presence of escalating doses of thrombomodulin. Data represents the mean ± SD of three separate experiments. (*K*) Tail-clip model of hemophilia type A mice (factor VIII deficient). Mice ($n = 5$) were pretreated by intravenous injection with SERPIN variants 5 min prior to the tail clip. Data are represented as scatterplots with medians. ns: not significant, $^{***}P = 0.0001$, and $^{****}P < 0.0001$ by one-way ANOVA with post hoc Tukey multiple comparison test.

that the anticoagulant function of APC is only partly responsible for the observed bleeding tendency in hemophilia A mice. Interestingly, a similar observation was observed in this FVIII-deficient model when treated with emicizumab, which also required infusion with human FIX and FX for species compatibility (33). However, in the presence of low-FVIII concentrations, emicizumab was able to completely restore blood loss. Although this requires further investigation, it may suggest that low levels of FVIII (as present in part of the human hemophilia A patients) could further enhance the therapeutic effects of APC-specific SERPINs.

While the efficacy of α1AT-KR/K has been assigned to its ability to inhibit APC, it is also a potent inhibitor of plasmin (Fig. 3*E*). This allows α1AT-KR/K to protect the formed fibrin from the degradation in clot lysis assays (*SI Appendix*, Fig. S16). We found that α1AT-KMPR/RIRA was superior to α1AT-KR/K in our tail-clip model, despite the higher-antifibrinolytic activity of the latter (Fig. 4*K*). It is important to note that plasmin contributes to bleeding in hemophilia in selective tissues: Antifibrinolytic therapy predominantly attenuates bleeding in mucosal areas of hemophilia patients (34, 35). Conversely, these agents are ineffective in other tissues (36). Indeed, the tail-clip bleeding model is sensitive to defects in primary hemostasis. Since thrombin is a powerful platelet activator, the modulation of thrombin formation is likely to impact this model, explaining our findings.

Besides its anticoagulant role (through cofactor inactivation), APC has effects on endothelial barrier stabilization and has anti-apoptotic and anti-inflammatory properties (through PAR-1 cleavage) (37, 38). Recently, an antibody against APC was developed that normalized hemostasis in vivo but did not interfere with these cytoprotective functions (39). Future studies may uncover whether APC-inhibiting SERPINs also inhibit these cytoprotective functions.

Compared to monoclonal antibodies, the circulation half-life of SERPINs is short: WT-α1AT; 4.5 d [in humans (40)] and recombinant α1AT; 46.9 min [in mice (41)]. As such, patients with hemophilia would require repeated infusions with these APC-inhibiting SERPINs when continuous treatment is required. To overcome this obstacle, the in vivo expression of modified SERPINs might prove beneficial. There is experience in this area: In mice, the in vivo expression of α1AT-WT (for treatment of α1AT deficiency) has already achieved levels of 1,826 ± 201 μg/mL (42). However, a peak concentration of only 21 to 36 μg/mL has been achieved in humans (43). This is far below the required therapeutic level of 527 μg/mL. One way to lower the required therapeutic levels for SERPIN-based therapy could be to further increase their efficacy through RCL redesign.

In conclusion, we demonstrate a strategy to predict SERPIN RCL specificity. The prediction platform provides primary insights into SERPIN RCL sequence–function relationship toward selected proteases. As a showcase, we made use of the platform to enhance the development of next-generation, APC-specific SERPINs. Though, this concept should hold value more broadly by targeting proteases beyond those involved in the hemostatic system.

Materials and Methods

For an extensive material list, please refer to *SI Appendix*.

Construction of α1-Antitrypsin Mutants. The complementary DNA sequence of SERPINA1 that encodes α1AT-WT was obtained from the National Center for Biotechnology Information reference sequence (NM_001127707.1). The signal peptide sequence was replaced by an *EcoRI* digestion site and the tobacco etch virus protease cleavage site. After the naturally occurring stop codon, a *NotI* digestion site, was placed and the entire construct was obtained as a custom gene via integrated DNA technologies. The SERPINA1 sequence was digested from the vector via *EcoRI* and *NotI* and ligated into the digested pSM2 vector that encodes for an N-terminal Igκ secretion signal and two STREP-tags for protein purification (17, 44). A dedicated SERPINA1-*BsmBI* pSM2 expression vector was created by removing the C-terminal part of SERPINA1 via digestion by *BstEII* and *NotI* and replacing by a double-stranded DNA fragment (integrated DNA technologies) encoding the C-terminal part of SERPINA1. In this construct, the nucleotide sequence encoding P4 to P4′ residue was replaced with a random nucleotide sequence (327 bp) flanked by two *BsmBI* restriction sites. The SERPINA1-*BsmBI* pSM2 vector was digested with *BsmBI* in a presence of 1 mM DTT at 37 °C for 2 h. The desired P4′ to P4 nucleotide sequence for SERPINA1 mutants was created as an oligonucleotide duplex by annealing complementary forward custom-made primer and reverse custom-made primer (100 μM/primer) (*SI Appendix*, Tables S1 and S3) in T4 ligase buffer (50 mM Tris·HCl, 10 mM $MgCl_2$, 1 mM ATP, 10 mM DTT, and pH 7.5) in a presence of T4 Polynucleotide Kinase (5 units). The complementary primers were incubated in 37 °C for 30 min, after which the temperature was raised to 95 °C and incubated for 5 min. Sample temperature was reduced to 25 °C with a ramp rate of 5 °C/min to allow for proper primer–duplex formation. The oligonucleotide duplex was diluted in H_2O (1:200), and 1 μL diluted oligo duplex was ligated into 50 ng digested SERPINA1-*BsmBI* pSM2 vector via T4 DNA ligase. Constructs were confirmed by sequencing.

SERPIN–RCL Library Small-Scale Expression. A total of 2 mL HEK293 Freestyle cells (1.1×10^6 cells/mL) were transfected with 1 μg/mL of plasmid, encoding α1AT mutants via 293Fectin according to manufacturer instructions. After 4 d the supernatant was collected via centrifugation (2,000 rpm for 5 min). All samples of a library were produced in a single batch, including α1AT-WT and empty pSM2 vector as controls. The α1AT protein levels were assayed via SDS-PAGE separation and visualized via Coomassie Blue staining. α1AT protein bands (52 kDa) were quantified via the Odyssey infrared imager from LI-COR. Based upon the quantification, the samples' protein levels were equalized by diluting the samples with conditioned culture media, resulting in equal α1AT levels in each library. The equalized supernatants were stored at −20 °C.

SERPIN–RCL Library Inhibition Screening. For testing the inhibitory capacity of the α1AT mutants, the equalized supernatant was thawed at 37 °C and tested via chromogenic assays. A total of 0.2% (wild-type/volume) bovine serum albumin (BSA) in Hepes-buffered saline (HBS; 10 mM Hepes, 150 mM NaCl, and pH7.4). All the reagents were prewarmed to 37 °C prior to the experiment. α1AT supernatant was added to a 96-well vinyl assay plate (prewarmed to 37 °C), to which 10 μL protease of interest (*SI Appendix*, Table S4) was added to α1AT supernatants and incubated for 5 min. Afterward, 10 μL chromogenic substrate (0.5 mM final concentration) was added to the mixture. Substrate conversion was immediately monitored every 30 s by a SpectraMax M2e plate reader at 37 °C. For thrombin and plasmin activity assays, the conversion of the substrate was measured via fluorescence (excitation/emission: 360/480 nm). For FXa, FXIa, αFXIIa, PKa, and APC activity assays, the substrate conversion was measured via absorbance at 405 nm. Relative fluorescent units (RFU) or optical density (OD) after 15 min (t = 15) were used for data analysis. After equalization for SERPIN concentration (described in *SERPIN–RCL Library Small-Scale Expression*), all libraries were titrated into screening experiments for each protease so that 5 to 25% of the protease activity (relative to uninhibited protease) remained in the presence of the best-performing α1AT variant in that library. In this way, we avoided comparison under saturating conditions. We normalized the absolute effect of the best-performing variant as 100% inhibition to enable comparison.

Generation of RCL Prediction Score. In each library, the substrate conversion was converted to normalized protease inhibition score for each variant ($Score_{position}^{Amino\ acid}$) as follows:

$$Score_{position}^{Amino\ acid} = \frac{1 - \left(RFU\ or\ OD_{position}^{Amino\ acid\ at\ t=15}\right)}{1 - \left(\frac{Y}{X}\right)} \times 100,$$

where X = RFU or OD of α1AT-WT at t = 15 min, Y = RFU or OD of the strongest α1AT mutant in the library at t = 15 min. To score an α1AT RCL sequence, the normalized protease inhibition scores of P4 to P4′ were compounded as follows:

$$RCL\ prediction\ score = \left(\frac{Score_{P4}^{Amino\ acid}}{100} \times \frac{Score_{P3}^{Amino\ acid}}{100} \times \frac{Score_{P2}^{Amino\ acid}}{100} \times \cdots \times \frac{Score_{P4'}^{Amino\ acid}}{100}\right) \times 100.$$

SERPIN-Based Prediction Model Validation. Per target protease, a validation test–cohort (*SI Appendix*, Fig. S2*A*) was created which consists of α1AT mutants selected based on predictions from either the α1AT RCL library or

PS-SCL data (12, 13). From the α1AT RCL library, 10 top-scoring P2 and P3 residue combinations were selected as donor RCL sequences for α1-antitrypsin RCL variants. For comparative prediction studies, we indexed historical, published PS-SCL data to determine candidate donor sequences. Hereto, we converted PS-SCL data (presented as colored three-point scale in refs. (12 and 13) into a numerical value: 0 = no substrate conversion, 1 = intermediate substrate conversion, and 2 = strong substrate conversion (example for APC; *SI Appendix*, Fig. S2*B*). We subsequently ranked individual amino acids on each position by favorability for inhibiting a target protease based on their cumulative score (i.e., a high score signifies that it combines well with various neighboring amino acids; indicated in the axes of *SI Appendix*, Fig. S2*B*). Next, we normalized these cumulative scores (highest possible value = 100%) and combined normalized scores of P2 and P3 residues to obtain combinations of P2 and P3 residues that should be favorable (*SI Appendix*, Fig. S2*C*; P1 was fixed to be an R). The 10 highest ranking P2 and P3 combinations were selected as donor RCL sequences for mutants. Another 10 P2 and P3 combinations with the biggest score differences between α1AT RCL library and PS-SCL were selected. Eventually, all 30 selected combinations were pooled into a test–cohort (*SI Appendix*, Fig. S2*D* and Table S2), in which duplicate RCL sequences were excluded. In a blinded manner, another researcher expressed the test–cohort in a single batch and determined protease inhibition, as described in *SERPIN–RCL Library Inhibition Screening*. Data were plotted and analyzed in Prism Graphpad 7.02 software. A simple linear regression model was used to assess sample correlations.

Production and Purification of α1-Antitrypsin Variants. The SERPINA1 sequences that encode α1AT-WT, α1AT-KR/K, α1AT-KMPR/RIRA, α1AT-KIPR/RIRA, and α1AT-KRPR/RIRA were digested from pSM2 vector via *HindIII* and *NotI* and ligated into the digested pcDNA5FRT/TO vector. A total of 2.5×10^5 cells/mL of Flp-In T-REx 293 cells were seeded in a 24-well plate and cultivated in Dulbecco's modified Eagle's medium (DMEM; 10% volume/volume fetal bovine serum supplemented) for 24 h. Afterward, the cells were cotransfected with SERPINA1 variant in pcDNA5/FRT/TO vector (in a 1:9 ratio with the pOG44 Flp–recombinase expression vector) via Lipofectamine 3000 reagent, according to manufacturer instructions. Around 4 d after transfection, transfected cell lines were selected by 100 μg/mL hygromycin. Stable transfected cell lines were seeded in Corning HYPERFlask cell culture vessels (Merck) and cultivated for 7 d to reach confluency. After which, protein expression was induced by replacing old culture media with doxycycline supplemented DMEM (DMEM + Ultroser G, 1,000 U/mL penicillin–streptomycin, 10 μg/mL blasticidin, 100 μg/mL hygromycin B, and 1 μg/mL doxycycline). After 7 d, the supernatant was collected. Cell debris was removed via centrifugation (5,000× *g* for 15 min). Supernatant was concentrated and dialyzed against STREP buffer (100 mM Tris-HCL, 150 mM NaCl, 1 mM EDTA, and pH = 8) via a QuixStand Benchtop system. Recombinant α1AT and variants were purified from the concentrate by strep–tactin Sepharose beads according to manufacturer instructions (IBA Lifesciences). For in vivo studies, purified α1AT variants were further purified via gel filtration over a HiPrep 26/10 Desalting column (GE Healthcare) with endotoxin-free phosphate-buffered saline (21 mM Na_2HPO_4, 2.8 mM NaH_2HPO_4, 140 mM NaCl, and pH = 7.4). Protein concentrations were determined via absorption spectroscopy at OD_{280nm}. Absorption coefficients were determined via ProtParam (45). Purity was assessed via 4 to 12% Bis-Tris–PAGE gel and Coomassie Blue staining. Purified α1AT variants were stored at −80 °C.

Protease Inhibition with Purified α1-Antitrypsin. Purified proteases and α1AT variants were diluted (in 0.2% [wild-type/volume] BSA-HBS, pH = 7.4) to 2.5× of their desired in-assay concentrations. A total of 20 μL protease (final concentration = 17.8 nM APC, 8.9 nM thrombin, 8.7 nM FXa, 2.5 nM FXIa, 25 nM FXIIa, 1 nM PKa, and 24.1 nM plasmin) was incubated with 20 μL α1AT variant or vehicle for 5 to 30 min at 37 °C in a 96-well assay plate. Hereafter, 10 μL of chromogenic or fluorogenic substrate was added, and conversion (absorbance: 405 nm; fluorescence: excitation, 380 nm and emission, 460 nm) was monitored for 30 min at 37 °C.

Determination of Inhibition Rate Constants. Second-order rate constants were determined via a discontinuous method under pseudo–first-order conditions (18). Both the α1AT and proteases were diluted in assay buffer (20 mM Tris pH 7.4, 100 mM NaCl, 2.5 mM $CaCl_2$, 0.2% wild-type/volume BSA, and 0.1% wild-type/volume PEG 8000). Each target protease was preincubated with a concentration range of α1AT at 37 °C. Per concentration, eight preincubation time points were determined, including 0 min. To stop the preincubation, a chromogenic substrate was added, and the residual enzymatic activity was determined. Slopes were determined from the linear part of the chromogenic substrate conversion, transformed into their respective natural log value, and plotted over time. From the slope of this plot, the apparent first-order constant k_{obs} was calculated and plotted against five different α1AT concentrations (*SI Appendix*, Table S5). The slope of this linear plot gave the second-order rate constant $k_2 \pm$ the SD of the slope.

Thrombin Generation Assays. Thrombin generation was performed as published (46). Briefly, 60 μL of human normal pooled citrated plasma was incubated with 20 μL purified α1AT variant in 0.2% wild-type/volume BSA-HBS and 10 μL vehicle or thrombomodulin (0, 1.25, 5, or 10 nM) at 37 °C for 5 min. Hereafter, 20 μL activator was added (4 μM phospholipid vesicles and 0.5 pM TF). Coagulation was initiated by the addition of 10 μL FluCa (17.5 mM Hepes, 16.67 mM $CaCl_2$, 0.42 mM Gly-Gly-Arg-AMC, 5.25% wild-type/volume BSA, and pH = 7.4). Substrate conversion was measured at 380 nm excitation and 460 nm emission wavelengths and monitored for at least 90 min at 37 °C. For calibration, the activator was replaced by thrombin–α2-macroglobulin complex (Thrombin calibrator) in the absence of α1AT. The obtained data were converted into thrombin generation peaks via Thrombinoscope software (Synapse). To assess thrombin generation in FVIII- or FIX-deficient plasma, thrombin generation was performed as described earlier except that 1 and 4 pM TF was used for FVIII-deficient plasma and FIX-deficient plasma, respectively.

To assess thrombin generation in mouse plasma, 20 μL citrated plasma of healthy C57BL/6 mice was incubated with 20 μL purified α1AT in 0.2% wild-type/volume BSA-HBS and 10 μL vehicle or 25 nM thrombomodulin at 37 °C for 5 min. Hereafter, 10 μL activator was added (4 μM phospholipid vesicles and 0.8 pM TF). Coagulation was initiated by the addition of 5 μL FluCa. Substrate conversion was measured at 380 nm excitation and 460 nm emission wavelengths and monitored for at least 60 min at 37 °C.

Clot Lysis Assay. Clot lysis was assessed in human normal, pooled citrated plasma, FVIII-deficient plasma or FIX-deficient plasma. A total of 60 μL plasma was incubated with 10 μL purified α1AT variant (final concentration 1 μM) in 0.2% wild-type/volume BSA-HBS and 10 μL tPA (final concentration 6 nM). In addition, 10 μL vehicle or 5 nM thrombomodulin was added and incubated at 37 °C for 5 min. Hereafter, 20 μL activator was added (4 μM phospholipid vesicles and 0.5 pM TF). Coagulation was initiated by an addition of 16.67 mM $CaCl_2$. Fibrin clot formation and lysis were monitored kinetically via light absorbance at 405 nm for 2 h at 37 °C.

To assess clot lysis in FVIII- or FIX-deficient plasma, clot lysis was performed as described earlier, except that 1 and 4 pM TF was used for FVIII-deficient plasma and FIX-deficient plasma, respectively.

Dilute PT. The PT was determined with the Dade Innovin reagent. The Dade Innovin was reconstituted as described by the manufacturer; hereafter, it was diluted 1,000-fold in $CaCl_2$ (16.6 mM). Normal pooled plasma was supplemented with 3 μM α1AT. A total of 50 μL prewarmed plasma was mixed with 50 μL prewarmed, diluted Dade Innovin. Plasma coagulation times were measured on an MC10 plus coagulometer (Merlin Medical).

Dilute aPTT. The aPTT was determined via the Dade Actin FS reagent. The Dade Actin FS was diluted 16-fold in HBS. Normal pooled plasma was supplemented with 3 μM α1AT. A total of 50 μL prewarmed plasma was mixed with 50 μL prewarmed, diluted Dade Actin FS and incubated for 2 min. Hereafter, 50 μL prewarmed $CaCl_2$ (25 mM) was added, and plasma coagulation times were measured on an MC10 plus coagulometer (Merlin Meical).

Determination of SERPIN–Protease Complex Formations in Plasma. A total of 60 μL of human normal pooled citrated plasma was incubated with 1 μM purified α1AT variant in 0.2% wild-type/volume BSA-HBS and 5 nM thrombomodulin or vehicle at 37 °C for 5 min. Hereafter, 20 μL activator was added (4 μM phospholipid vesicles and 0.5 pM TF). Coagulation was initiated by the addition of 16.67 mM $CaCl_2$. The samples were incubated at 37 °C for 60 min. After which, samples were mixed with 3× sample buffer (SB; 30% glycerol, 0.18 M Tris·HCl, 6% SDS, bromophenol blue, and in a presence of 25 mM DTT) and heated at 95 °C for 10 min. To assess plasmin complexation, 6 nM tPA or vehicle was added to 60 μL of human normal pooled citrated plasma prior to 1 μM purified α1AT variant and 5 nM thrombomodulin or vehicle incubation. Coagulation was initiated by the addition of 16.67 mM $CaCl_2$. The samples were incubated at 37 °C for 2 h. After which, samples were mixed with 3× SB (in a presence of 25 mM DTT) and heated at 95 °C for 10 min. Samples were separated on 4 to 12% Bis-Tris gels at 165V for 65 to 120 min in MOPS-SDS running buffer. Proteins were transferred to Immobilon–FL membranes at 125V for 55 min in blotting buffer (25 mM Tris, 192 mM glycine, and 20% [volume/volume] ethanol). Membranes were blocked for 2 h at room temperature (RT) with blocking buffer (Odyssey blocking reagent diluted 1:1 in Tris-buffered saline; TBS). Subsequently, the protein of interest was detected by an overnight incubation (at 4 °C) of the membranes with primary antibody (*SI Appendix*, Table

S7). Membranes were washed with 0.05% (volume/volume) tween in TBS (TBS-T), and primary antibody was detected with corresponding secondary antibody for 1 h at RT. Membranes were washed with TBS-T and analyzed on a near-infrared Odyssey scanner (LI-COR). Band densitometry was analyzed with Odyssey software (LI-COR).

Restoration of Clotting in Hemophilic Mice by SERPINs. The tail-clip model was performed as previously described (33) with approval of the local ethical committee of Université Paris-Sud (Comité d'Éthique en Expérimentation Animale No. 26, protocol APAFIS#4400–201602171643 1023v5). Briefly, FVIII-deficient mice (47) (backcrossed on a C57BL/6 strain) were anesthetized with isoflurane. Around 5 min prior to the tail amputation, mice were administered with the recombinant α1AT variants by intravenous injection via the retroorbital venous plexus. Subsequently, 3 mm of the distal tip of the tail was amputated, and the tail was immersed in prewarmed physiological saline (37 °C) for 30 min. Hereafter, the sample was centrifuged at 1,500× *g* for 20 min. The red blood cell pellet was lysed by resuspension in H_2O, and hemoglobin levels were quantified at 416 nm. Blood loss was calculated from a standard curve by lysing defined amounts of mouse red blood cells in distilled H_2O.

Data Availability. All study data are included in the article and/or *SI Appendix*.

ACKNOWLEDGMENTS. W.S. gratefully acknowledges a full PhD scholarship from the Royal Thai Government. S.d.M. gratefully acknowledges the Toegepaste en Technische Wetenschappen (TTW) section of The Netherlands Organization for Scientific Research (2019/TTW/00704802). P.J.L. and T.S. gratefully acknowledge funding from Sobi. We thank Dougald Monroe for valuable advice concerning the in vivo study.

1. L. Hedstrom, Serine protease mechanism and specificity. *Chem. Rev.* **102**, 4501–4524 (2002).
2. W. Sanrattana, C. Maas, S. de Maat, SERPINs-From trap to treatment. *Front. Med. (Lausanne)* **6**, 25 (2019).
3. P. G. W. Gettins, S. T. Olson, Exosite determinants of serpin specificity. *J. Biol. Chem.* **284**, 20441–20445 (2009).
4. H. Loebermann, R. Tokuoka, J. Deisenhofer, R. Huber, Human α 1-proteinase inhibitor. Crystal structure analysis of two crystal modifications, molecular model and preliminary analysis of the implications for function. *J. Mol. Biol.* **177**, 531–557 (1984).
5. J. A. Huntington, R. J. Read, R. W. Carrell, Structure of a serpin-protease complex shows inhibition by deformation. *Nature* **407**, 923–926 (2000).
6. E. Stratikos, P. G. Gettins, Formation of the covalent serpin-proteinase complex involves translocation of the proteinase by more than 70 A and full insertion of the reactive center loop into β-sheet A. *Proc. Natl. Acad. Sci. U.S.A.* **96**, 4808–4813 (1999).
7. J. A. Huntington, R. W. Carrell, The serpins: Nature's molecular mousetraps. *Sci. Prog.* **84**, 125–136 (2001).
8. C. F. Scott *et al.*, Alpha-1-antitrypsin-Pittsburgh. A potent inhibitor of human plasma factor XIa, kallikrein, and factor XIIf. *J. Clin. Invest.* **77**, 631–634 (1986).
9. P. Goettig, H. Brandstetter, V. Magdolen, Surface loops of trypsin-like serine proteases as determinants of function. *Biochimie* **166**, 52–76 (2019).
10. M. C. Owen, S. O. Brennan, J. H. Lewis, R. W. Carrell, Mutation of antitrypsin to antithrombin. alpha 1-antitrypsin Pittsburgh (358 Met leads to Arg), a fatal bleeding disorder. *N. Engl. J. Med.* **309**, 694–698 (1983).
11. H. Rubin *et al.*, Conversion of α 1-antichymotrypsin into a human neutrophil elastase inhibitor: Demonstration of variants with different association rate constants, stoichiometries of inhibition, and complex stabilities. *Biochemistry* **33**, 7627–7633 (1994).
12. D. N. Gosalia, C. M. Salisbury, D. J. Maly, J. A. Ellman, S. L. Diamond, Profiling serine protease substrate specificity with solution phase fluorogenic peptide microarrays. *Proteomics* **5**, 1292–1298 (2005).
13. D. N. Gosalia, C. M. Salisbury, J. A. Ellman, S. L. Diamond, High throughput substrate specificity profiling of serine and cysteine proteases using solution-phase fluorogenic peptide microarrays. *Mol. Cell. Proteomics* **4**, 626–636 (2005).
14. J. L. Harris, E. P. Peterson, D. Hudig, N. A. Thornberry, C. S. Craik, Definition and redesign of the extended substrate specificity of granzyme B. *J. Biol. Chem.* **273**, 27364–27373 (1998).
15. J. L. Harris *et al.*, Rapid and general profiling of protease specificity by using combinatorial fluorogenic substrate libraries. *Proc. Natl. Acad. Sci. U.S.A.* **97**, 7754–7759 (2000).
16. S. L. Ivry *et al.*, Global substrate specificity profiling of post-translational modifying enzymes. *Protein Sci.* **27**, 584–594 (2018).
17. S. de Maat *et al.*, Design and characterization of α1-antitrypsin variants for treatment of contact system-driven thromboinflammation. *Blood* **134**, 1658–1669 (2019).
18. S. G. I. Polderdijk *et al.*, Design and characterization of an APC-specific serpin for the treatment of hemophilia. *Blood* **129**, 105–113 (2017).
19. S. G. I. Polderdijk, J. A. Huntington, Identification of serpins specific for activated protein C using a lysate-based screening assay. *Sci. Rep.* **8**, 8793 (2018).
20. E. W. Davie, O. D. Ratnoff, Waterfall sequence for intrinsic blood clotting. *Science* **145**, 1310–1312 (1964).
21. D. A. Lane, H. Philippou, J. A. Huntington, Directing thrombin. *Blood* **106**, 2605–2612 (2005).
22. C. T. Esmon, The protein C anticoagulant pathway. *Arterioscler. Thromb.* **12**, 135–145 (1992).
23. F. Simão, T. Ustunkaya, A. C. Clermont, E. P. Feener, Plasma kallikrein mediates brain hemorrhage and edema caused by tissue plasminogen activator therapy in mice after stroke. *Blood* **129**, 2280–2290 (2017).
24. P. C. Hopkins, D. C. Crowther, R. W. Carrell, S. R. Stone, Development of a novel recombinant serpin with potential antithrombotic properties. *J. Biol. Chem.* **270**, 11866–11871 (1995).
25. X. Xia, Z. Xie, Protein structure, neighbor effect, and a new index of amino acid dissimilarities. *Mol. Biol. Evol.* **19**, 58–67 (2002).
26. M. Fu, Z. Huang, Y. Mao, S. Tao, Neighbor preferences of amino acids and context-dependent effects of amino acid substitutions in human, mouse, and dog. *Int. J. Mol. Sci.* **15**, 15963–15980 (2014).
27. C. J. Crasto, J. Feng, Sequence codes for extended conformation: A neighbor-dependent sequence analysis of loops in proteins. *Proteins* **42**, 399–413 (2001).
28. H. M. Fooks, A. C. R. Martin, D. N. Woolfson, R. B. Sessions, E. G. Hutchinson, Amino acid pairing preferences in parallel β-sheets in proteins. *J. Mol. Biol.* **356**, 32–44 (2006).
29. P. C. Hopkins, R. N. Pike, S. R. Stone, Evolution of serpin specificity: Cooperative interactions in the reactive-site loop sequence of antithrombin specifically restrict the inhibition of activated protein C. *J. Mol. Evol.* **51**, 507–515 (2000).
30. E. M. Marijanovic *et al.*, Reactive centre loop dynamics and serpin specificity. *Sci. Rep.* **9**, 3870 (2019).
31. B. M. Scott *et al.*, Phage display of the serpin alpha-1 proteinase inhibitor randomized at consecutive residues in the reactive centre loop and biopanned with or without thrombin. *PLoS One* **9**, e84491 (2014). Correction in: *PLoS One* **15**, e0238969 (2020).
32. V. Bhakta *et al.*, Identification of an alpha-1 antitrypsin variant with enhanced specificity for factor XIa by phage display, bacterial expression, and combinatorial mutagenesis. *Sci. Rep.* **11**, 5565 (2021).
33. S. Ferrière *et al.*, A hemophilia A mouse model for the in vivo assessment of emicizumab function. *Blood* **136**, 740–748 (2020).
34. C. D. Forbes *et al.*, Tranexamic acid in control of haemorrhage after dental extraction in haemophilia and Christmas disease. *Br. Med. J* **2**, 311–313 (1972).
35. M. J. Coetzee, The use of topical crushed tranexamic acid tablets to control bleeding after dental surgery and from skin ulcers in haemophilia. *Haemophilia* **13**, 443–444 (2007).
36. R. Stagaard *et al.*, Abrogating fibrinolysis does not improve bleeding or rFVIIa/rFVIII treatment in a non-mucosal venous injury model in haemophilic rodents. *J. Thromb. Haemost.* **16**, 1369–1382 (2018).
37. J. H. Griffin, B. V. Zlokovic, L. O. Mosnier, Activated protein C: Biased for translation. *Blood* **125**, 2898–2907 (2015).
38. L. O. Mosnier, B. V. Zlokovic, J. H. Griffin, The cytoprotective protein C pathway. *Blood* **109**, 3161–3172 (2007).
39. X.-Y. Zhao *et al.*, Targeted inhibition of activated protein C by a non-active-site inhibitory antibody to treat hemophilia. *Nat. Commun.* **11**, 2992 (2020).
40. J. E. Gadek, H. G. Klein, P. V. Holland, R. G. Crystal, Replacement therapy of alpha 1-antitrypsin deficiency. Reversal of protease-antiprotease imbalance within the alveolar structures of PiZ subjects. *J. Clin. Invest.* **68**, 1158–1165 (1981).
41. A. Lusch *et al.*, Development and analysis of alpha 1-antitrypsin neoglycoproteins: The impact of additional N-glycosylation sites on serum half-life. *Mol. Pharm.* **10**, 2616–2629 (2013).
42. M. L. Sosulski *et al.*, Gene therapy for alpha 1-antitrypsin deficiency with an oxidant-resistant human alpha 1-antitrypsin. *JCI Insight* **5**, e135951 (2020).
43. T. R. Flotte *et al.*, Phase 2 clinical trial of a recombinant adeno-associated viral vector expressing α1-antitrypsin: Interim results. *Hum. Gene Ther.* **22**, 1239–1247 (2011).
44. S. de Maat *et al.*, Plasmin is a natural trigger for bradykinin production in patients with hereditary angioedema with factor XII mutations. *J. Allergy Clin. Immunol.* **138**, 1414–1423.e9 (2016).
45. M. R. Wilkins *et al.*, Protein identification and analysis tools in the ExPASy server. *Methods Mol. Biol.* **112**, 531–552 (1999).
46. H. C. Hemker *et al.*, Calibrated automated thrombin generation measurement in clotting plasma. *Pathophysiol. Haemost. Thromb.* **33**, 4–15 (2003).
47. L. Bi *et al.*, Targeted disruption of the mouse factor VIII gene produces a model of haemophilia A. *Nat. Genet.* **10**, 119–121 (1995).